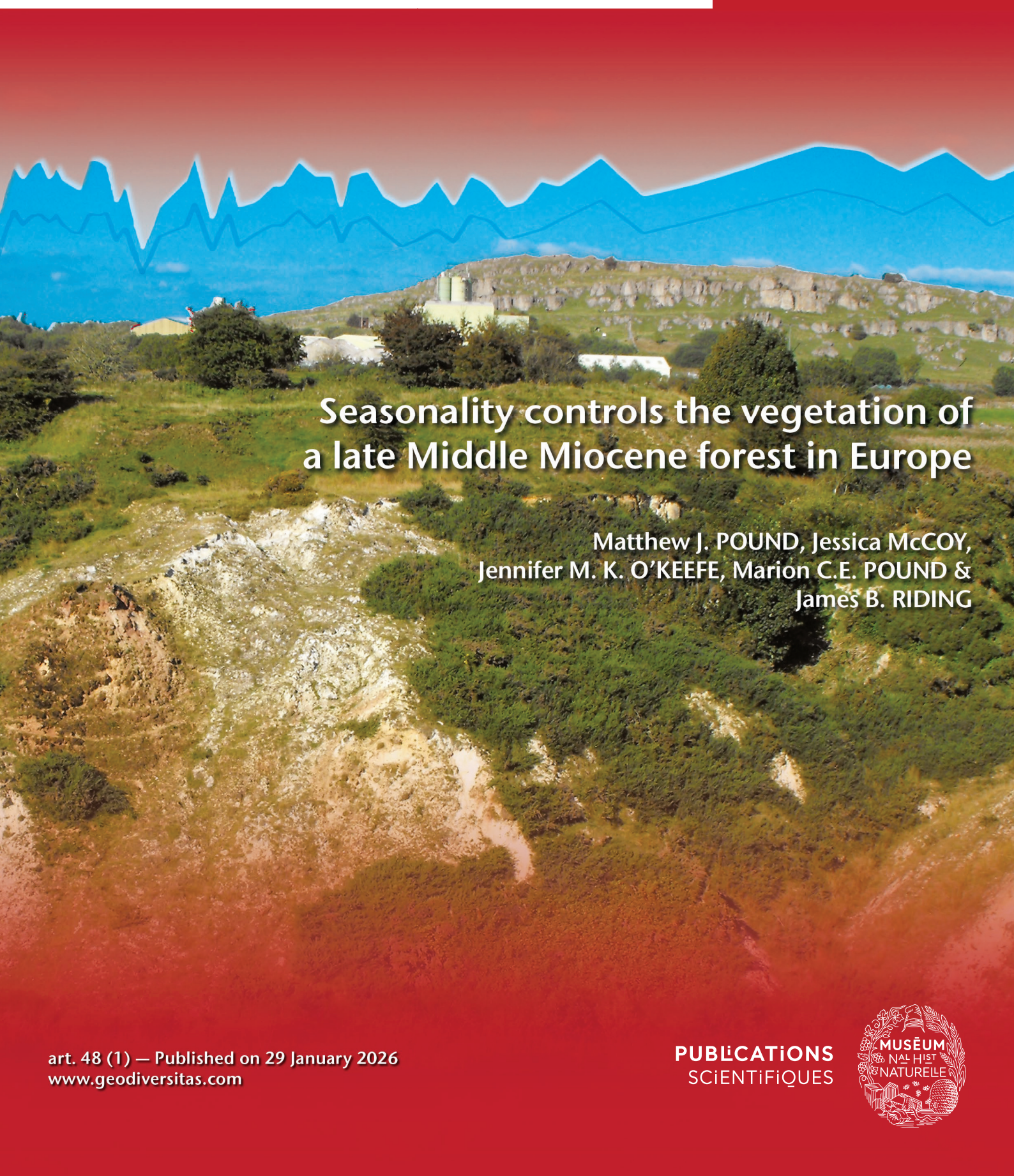


geodiversitas

2026 • 48 • 1



Seasonality controls the vegetation of
a late Middle Miocene forest in Europe

Matthew J. POUND, Jessica MCCOY,
Jennifer M. K. O'KEEFE, Marion C.E. POUND &
James B. RIDING

DIRECTEUR DE LA PUBLICATION / *PUBLICATION DIRECTOR* : Gilles Bloch,
Président du Muséum national d'Histoire naturelle

RÉDACTEUR EN CHEF / *EDITOR-IN-CHIEF*: Sylvain Charbonnier

RÉDACTEUR ASSOCIÉ / *ASSOCIATE EDITOR*: Didier Merle

ÉDITEUR TECHNIQUE (SUIVI ÉDITORIAL) / *DESK EDITOR (EDITORIAL PROCESS)*: Emmanuel Côtez (geodiv@mnhn.fr)

ÉDITEUR TECHNIQUE (PRODUCTION) / *DESK EDITOR (PRODUCTION)*: Emmanuel Côtez

COMITÉ SCIENTIFIQUE / *SCIENTIFIC BOARD*:

Christine Argot (Muséum national d'Histoire naturelle, Paris)
Beatrix Azanza (Museo Nacional de Ciencias Naturales, Madrid)
Raymond L. Bernor (Howard University, Washington DC)
Henning Blom (Uppsala University)
Gaël Clément (Muséum national d'Histoire naturelle, Paris)
Ted Daeschler (Academy of Natural Sciences, Philadelphie)
Cédric Del Rio (Muséum national d'Histoire naturelle)
Gregory D. Edgecombe (The Natural History Museum, Londres)
Ursula Gölich (Natural History Museum Vienna)
Jin Meng (American Museum of Natural History, New York)
Brigitte Meyer-Berthaud (CIRAD, Montpellier)
Zhu Min (Chinese Academy of Sciences, Pékin)
Isabelle Rouget (Muséum national d'Histoire naturelle, Paris)
Sevket Sen (Muséum national d'Histoire naturelle, Paris, retraité)
Stanislav Štamberg (Museum of Eastern Bohemia, Hradec Králové)
Paul Taylor (The Natural History Museum, Londres, retraité)

COUVERTURE / *COVER*:

Réalisée à partir des Figures de l'article/*Made from the Figures of the article*.

Geodiversitas est indexé dans / *Geodiversitas* is indexed in:

- Science Citation Index Expanded (SciSearch®)
- ISI Alerting Services®
- Current Contents® / Physical, Chemical, and Earth Sciences®
- Scopus®

Geodiversitas est distribué en version électronique par / *Geodiversitas* is distributed electronically by:

- BioOne® (<http://www.bioone.org>)

Les articles ainsi que les nouveautés nomenclaturales publiés dans *Geodiversitas* sont référencés par /
Articles and nomenclatural novelties published in Geodiversitas are referenced by:

- ZooBank® (<http://zoobank.org>)

Geodiversitas est une revue en flux continu publiée par les Publications scientifiques du Muséum, Paris
Geodiversitas is a fast track journal published by the Museum Science Press, Paris

Les Publications scientifiques du Muséum publient aussi / *The Museum Science Press also publish: Adansonia, Zoosystema, Anthropozoologica, European Journal of Taxonomy, Naturae, Cryptogamie sous-sections Algologie, Bryologie, Mycologie, Comptes Rendus Palevol*

Diffusion – Publications scientifiques Muséum national d'Histoire naturelle
CP 41 – 57 rue Cuvier F-75231 Paris cedex 05 (France)
Tél. : 33 (0)1 40 79 48 05 / Fax: 33 (0)1 40 79 38 40
diff.pub@mnhn.fr / <http://sciencepress.mnhn.fr>

Les articles publiés dans *Geodiversitas* sont distribués sous licence CC-BY 4.0/*Articles published in Geodiversitas are distributed under a CC-BY 4.0 license.*
ISSN (imprimé / print) : 1280-9659/ ISSN (électronique / electronic) : 1638-9395

Seasonality controls the vegetation of a late Middle Miocene forest in Europe

Matthew J. POUND
Jessica MCCOY

School of Geography and Natural Sciences,
Northumbria University, Newcastle upon Tyne NE1 8ST (United Kingdom)
matthew.pound@northumbria.ac.uk (corresponding author)
jessica.mccoy@northumbria.ac.uk

Jennifer M. K. O'KEEFE

Department of Engineering Sciences, Morehead State University,
Morehead, KY 40351 (United States of America)
j.okeefe@moreheadstate.edu

Marion C. E. POUND

Corbridge Middle School, Corbridge, Northumberland NE45 5HX (United Kingdom)
marion.pound@corbridgemiddle.co.uk

James B. RIDING

British Geological Survey, Keyworth, Nottingham NG12 5GG (United Kingdom)
jbri@bgs.ac.uk

Submitted on 22 November 2024 | accepted on 17 March 2025 | published on 29 January 2026

urn:lsid:zoobank.org:pub:52481C19-937C-4C0A-AE5B-78C0EAD650D8

Pound M. J., McCoy J., O'Keefe J. M. K., Pound M. C. E. & Riding J. B. 2026. — Seasonality controls the vegetation of a late Middle Miocene forest in Europe. *Geodiversitas* 48 (1): 1-13. <https://doi.org/10.5252/geodiversitas2026v48a1>. <http://geodiversitas.com/48/1>

ABSTRACT

The Miocene was a past warm interval considered highly relevant to future climate projections. Whilst temperatures during the Miocene were constrained by multiple proxies, the hydrology of the Miocene is still largely unknown. Here we present a new palaeoclimatic analysis of the Middle Miocene (Serravallian) Kenslow Member of the Brassington Formation in the United Kingdom to elucidate the hydrology of this interval. Using fossil palynomorphs we perform a Bayesian palaeoclimate reconstruction, plant functional type analysis and cluster analysis. Our results show that summer and winter precipitation were important factors in the dynamics of Miocene forests, even in a climate zone with no pronounced dry season.

KEY WORDS
Palaeoclimate,
United Kingdom,
Serravallian,
hydrology,
palynology.

RÉSUMÉ

La saisonnalité contrôle la végétation d'une forêt de la fin du Miocène moyen en Europe.

Le Miocène a été un intervalle chaud, considéré très important pour les projections climatiques du futur. Même si les températures du Miocène ont été contraintes par de multiples proxys, son hydrologie est toujours largement méconnue. Ici nous présentons une nouvelle analyse paléoclimatique du Membre de Kenslow (Miocène moyen, Serravallien) de la Formation Brassington au Royaume-Uni, pour comprendre l'hydrologie de cet intervalle. En utilisant des palynomorphes fossiles, nous réalisons une reconstitution paléoclimatique bayésienne, une analyse des types végétaux fonctionnels et une analyse en clusters. Nos résultats montrent que les précipitations estivales et hivernales constituaient des facteurs déterminants dans la dynamique des forêts du Miocène, même dans une zone climatique sans saison sèche marquée.

MOTS CLÉS

Paléoclimat,
Royaume-Uni,
Serravallien,
hydrologie,
palynologie.

INTRODUCTION

The Miocene is an important geological time interval for palaeoclimatic study (Steinthorsdottir *et al.* 2021). With elevated atmospheric carbon dioxide (CO_2) concentrations, near modern continental distribution and smaller polar glaciers, the processes, forcings and feedbacks that operated during this epoch are highly relevant to our understanding of the contemporary climate system (Steinthorsdottir *et al.* 2021; Forster *et al.* 2021; Gibson *et al.* 2022). Substantial attention has been paid to temperatures during the Miocene, but substantially less progress has been made in understanding the hydrology of this warmer world (Gibson *et al.* 2022; Acosta *et al.* 2024a). Focussing on Europe, precipitation during the Miocene has been investigated through mammals (van Dam 2006), herpetofaunas (Böhme *et al.* 2008), palaeobotany (Bruch *et al.* 2011), paleosol chemistry (Methner *et al.* 2020) and climate modelling (Botsyun *et al.* 2022). However, there is considerable disagreement between these proxies – both in terms of precipitation magnitude and inferred seasonality. Excluding the more arid Iberian Peninsula, mammals reconstruct precipitation values of 800–1300 mm/yr and palaeobotany reconstructs 850–1500 mm/yr (van Dam 2006; Bruch *et al.* 2011; McCoy *et al.* 2022). Herpetofaunas reconstruct values from 0 to 300 mm/yr (Böhme *et al.* 2008), which agrees with the modelling results of Botsyun *et al.* (2022), but not those of Acosta *et al.* (2024b). Here we present a new palaeoclimate reconstruction and palaeoenvironmental data for the Middle Miocene (Serravallian) Kenslow Member from the English East Midlands of the United Kingdom (Fig. 1).

The islands that make up the United Kingdom and Ireland have a unique position geographically and climatically. Positioned on the northern edge of the temperate zone, they experience a low degree of precipitation seasonality and, due to the influence of warm water currents, a substantially moderated temperature seasonality (Mayes 1996). Of the few sites in the onshore United Kingdom with Miocene age sediments, the Brassington Formation is by far the most extensive geographically and stratigraphically (Boulter *et al.*

1971; Walsh *et al.* 2018). Comprised of three members, so far only the uppermost Kenslow Member has yielded abundant palaeobotanical and palynological remains (Boulter *et al.* 1971; Walsh *et al.* 2018; O'Keefe *et al.* 2020; McCoy *et al.* 2022). The Kenslow Member is diachronous in age (ranging from Serravallian to Tortonian) due to its unique depositional setting in distinct karstic hollows (Pound & Riding 2016; Walsh *et al.* 2018).

Recent work on the oldest occurrence of the Kenslow Member at Bees Nest Pit (Fig. 1) has revealed an evolving forested wetland was present during the Serravallian (McCoy *et al.* 2022). Towards the base of the section a conifer forest was dominant, which shifted to a mixed mesophytic forest and finally a small open-canopy peat producing wetland at the top of section (McCoy *et al.* 2022). This change in the sedimentology, from clay to lignite, is also reflected in the fungal assemblage reported from this section (Fig. 1). In palynology samples taken from the lignite, there is an increase in the diversity and abundance of freshwater saprotrophic fungi (Pound *et al.* 2022). The Mean Annual Temperature (MAT) of the Serravallian Kenslow Member was reconstructed using the crestr and CRACLE packages on the palynology published by Pound & Riding (2016) as $13.7^\circ\text{C} \pm 0.3^\circ\text{C}$, and Mean Annual Precipitation (MAP) of around 1000 mm (Gibson *et al.* 2022). However, Gibson *et al.* (2022) could not confirm the lack of seasonality proposed by McCoy *et al.* (2022). Finally, in the first application of a fungal-based reconstruction technique, Pound *et al.* (2022) showed either a Cfa or Cfb Köppen-Geiger climate class was present during the Serravallian, suggesting no seasonality in rainfall, with either hot, or warm, summers.

The aim of this paper is to provide a new palaeoclimate reconstruction, plant functional type analysis and biome determination for the Kenslow Member flora that can resolve the uncertainties in the late Serravallian climate of the United Kingdom, and find a direction towards consensus in the late Middle Miocene hydrology of Europe. This has implications for our understanding of atmospheric circulation during this warmer than present time interval.

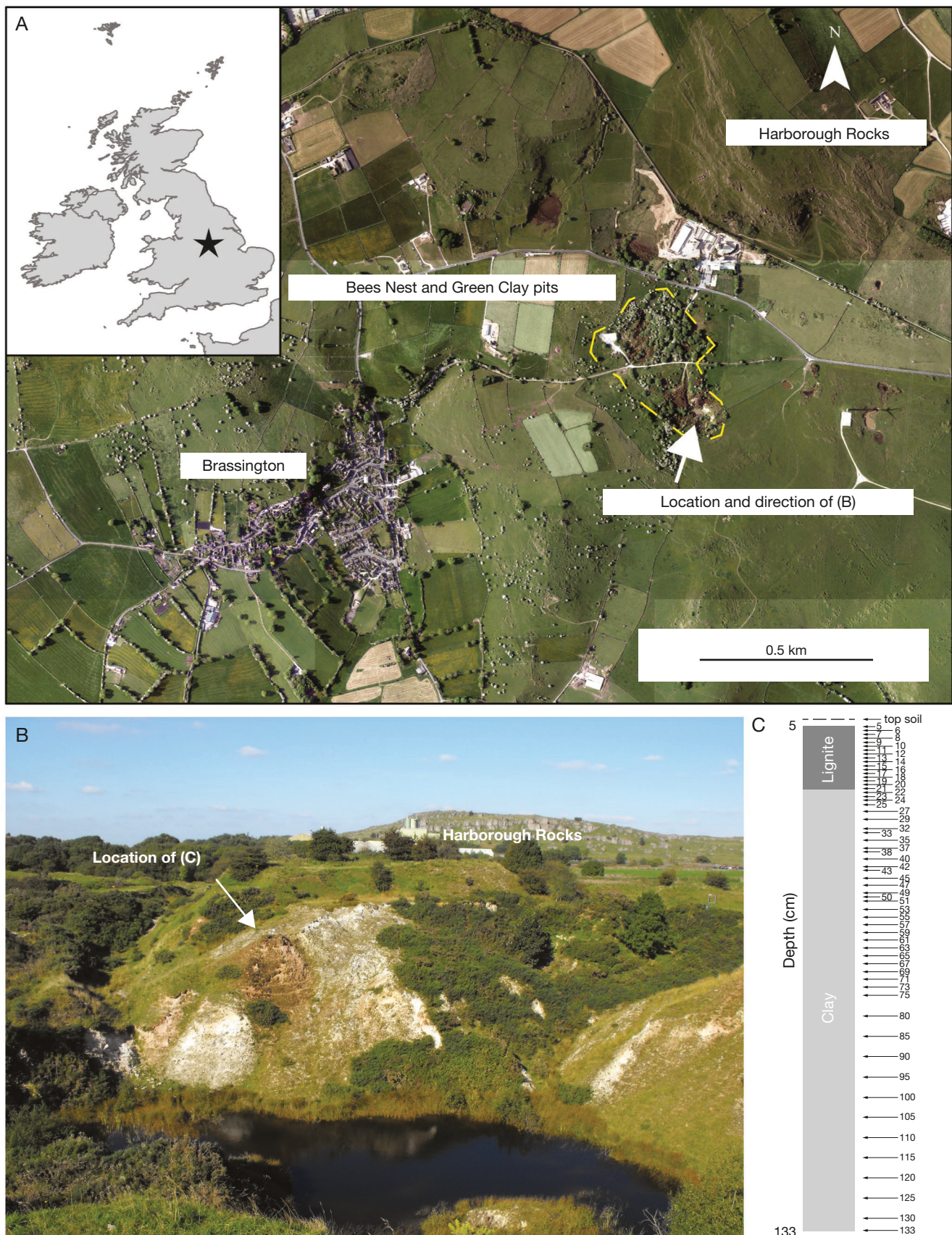


Fig. 1. — Location of the sampled Kenslow Member at the Bees Nest Pit: **A**, annotated aerial image of Bees Nest Pit near the village of Brassington, Derbyshire, United Kingdom. The inset map shows the location in the context of the United Kingdom, Ireland, France and the Faroe Islands; **B**, field photograph showing the location of the section with Harborough Rocks in the background; **C**, simplified stratigraphical column with sampling points indicated by arrows. Aerial images from Edina (2024). Photograph, author's own.

TABLE 1. — The five groups defined by cluster analysis and the plant palynomorphs that compose them. Taxonomy follows that originally presented in McCoy *et al.* (2022).

Group	Taxa
1	<i>Abiespollenites</i> , <i>Pinuspollenites</i> <i>Artemisia pollenites</i> , <i>Caprifoliaceae</i> , <i>Carpinites</i> , <i>Cathayapollenites</i> , <i>Iteapollenites</i> , <i>Keteleeria</i> , <i>Nyssapollenites</i> , <i>Oleidearumpollenites</i> , <i>Parthenopollenites</i> , <i>Platycaryapollenites</i> , <i>Rhamnaceae</i> , <i>Salixpollenites</i> , <i>Tetradomonoporites</i> , <i>Urtica</i> ,
2	<i>Verrucatosporites</i> , <i>Laevigatosporites</i> , <i>Echinatisporites</i> , <i>Stereisporites stroboides</i>
3	<i>Cercidiphyllum</i> , <i>Compositoipollenites</i> , <i>Coryloides</i> , <i>Cyperaceae</i> , <i>Ericipites</i> , <i>Ilexpollenites</i> , <i>Juglanspollenites</i> , <i>Oleidearumpollenites</i> , <i>Salixpollenites</i> , <i>Tricolpopollenites</i> sp.,
4	<i>Betulaepollenites</i> , <i>Cupressacites</i> , <i>Cupuliferoipollenites</i> , <i>Liliacidites</i> , <i>Sciadopitys</i> , <i>Tricopollenites liblarensis</i> , <i>Tricolpopollenites</i> <i>fallax</i> , <i>Quercoidites microhenrici</i> , <i>Zonalapollenites</i>
5	<i>Alnipollenites verus</i> , <i>Cedripites</i> , <i>Cyrillaceaepollenites</i> , <i>Graminidites</i> , <i>Myricipites</i> , <i>Piceaepollenites</i> , <i>Quercoidites henrici</i> , <i>Tricolpopollenites ipilensis</i> , <i>Tricolporopollenites</i> sp., <i>Lygodium</i>

MATERIAL AND METHODS

Using the 58 pollen assemblages from the KM-19 section of McCoy *et al.* (2022), we apply three techniques to reconstruct the biome and climate of the Kenslow Member flora from Bees Nest Pit. Full details of sampling location, geology and palynological processing are provided in McCoy *et al.* (2022). In brief, the section sampled was 133 cm in depth with present-day topsoil from 0 cm to 5 cm, lignite from 5 cm to 21 cm and clay with wood fossils for the remainder of the stratigraphy (Fig. 1). New quantitative palaeoclimate values are reconstructed using *crestr* (Chevalier 2022a). From these a Köppen-Geiger classification (Beck *et al.* 2018), Whittaker's biome classification (Whittaker 1970) and Holdridge's biome classification (Holdridge 1947) are defined. Using the same data, Plant Functional Types (Utescher *et al.* 2021a, b) and statistically defined groups (Pound & Salzmann 2017) are determined to reconstruct the sub-biome vegetation for the Kenslow Member and identify correlation between climate and vegetation.

QUANTITATIVE PALAEOCLIMATE RECONSTRUCTIONS

Crestr (Chevalier 2022a) was used to reconstruct Mean Annual Temperature (MAT), Mean Annual Precipitation (MAP), Mean Temperature of the Coldest Quarter (referred to hereafter as Winter Temperature), Mean Temperature of the Warmest Quarter (referred to hereafter as Summer Temperature), Mean Precipitation of the Warmest Quarter (referred to hereafter as Summer Precipitation) and Mean Precipitation of the Coldest Quarter (referred to hereafter as Winter Precipitation). *Crestr* takes the present-day geographical distributions of a fossil assemblages' nearest living relatives, and plots the climate space probability density functions of all taxa for each assemblage. From these, an optima, mean and uncertainty intervals can be defined (Chevalier *et al.* 2014; Chevalier 2019, 2022a). Present-day distribution data comes from GBIF (2020a-e), and climatology is from WorldClim2 (Fick & Hijmans 2017). The script follows the recommended parameterisation, using presence-absence of taxa and sampling the modern climate-

taxa space at a global level to account for the non-modern analogue nature of Miocene vegetation (Chevalier *et al.* 2014; Chevalier 2019, 2022a). The script is available from Chevalier (2022b). The script was run in RStudio (RStudio Team 2022) and results were plotted in MatLab. From these quantitative reconstructions, the mean values are used to determine a Koppen-Geiger classification (Beck *et al.* 2018; McCoy *et al.* 2024), Whittaker's biome (Whittaker 1970) and Holdridge's biome (Holdridge 1947). In presenting the results we focus on the mean value and 50% uncertainty intervals, but all data is presented in the supplementary information (SI 1).

PLANT FUNCTIONAL TYPES AND POLLEN GROUPS

The assignment of Plant Functional Types (PFTs) is based on nearest living relative principles and follows Utescher *et al.* (2021b). The count data of McCoy *et al.* (2022) was turned into a presence/absence matrix. Defining PFT proportions via raw count, or percentage data, would ignore differences in pollen production, pollination mode and dispersal between taxa (Prentice 1985; Escobar-Torrez *et al.* 2024). Taxa were assigned to one, or multiple, of 41 PFTs using François *et al.* (2011) and Utescher *et al.* (2021b). Where a taxon was assigned to more than one PFT, it was proportionally weighted so not to overemphasise uncertainty in assignment (Utescher *et al.* 2021a). Full PFT assignments are provided in the supplementary information (SI 2), but for the purposes of visualising the results, the 41 PFTs were then grouped based on shared characteristics (e.g. drought tolerance, broadleaved evergreen vs deciduous). Assigning reproductive propagules (pollen and spores) to a PFT has inherent limitations. The biggest of these applies to all nearest living relative approaches – the assumption of uniformitarianism and the applicability of a present-day taxon to one from the Miocene (Utescher *et al.* 2014). A related source of uncertainty, and of particular relevance to pollen and spores, is the assumption of particular traits (e.g. deciduous or evergreen leaf habit) based solely on nearest living relative assignment. Considering these limitations, an additional grouping of palynomorphs was made that did not rely on uniformitarianism. Pollen and spore count data from

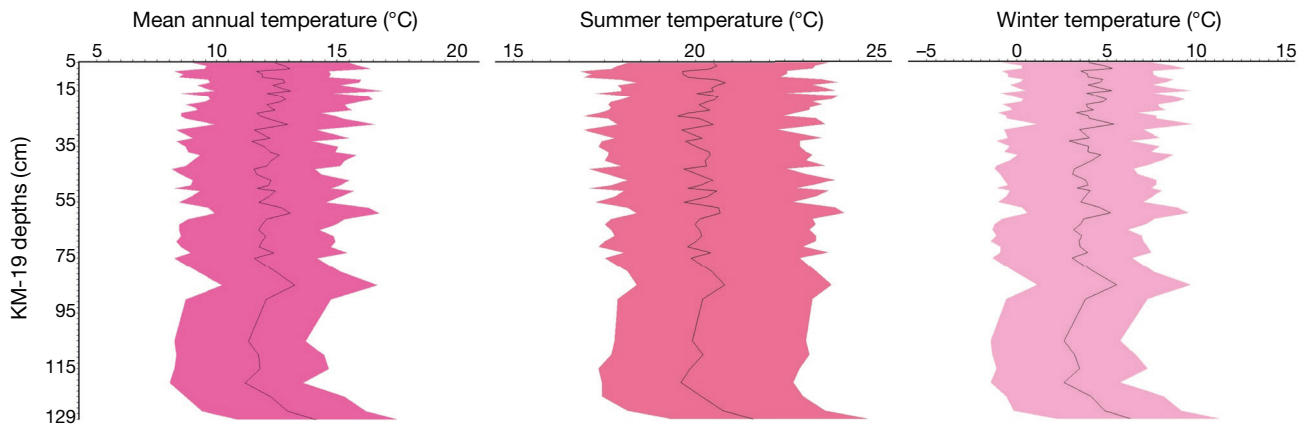


Fig. 2. — Temperature reconstructions of the Kenslow Member showing the mean value (black line) and 50% uncertainty intervals (coloured portions). The average values for the entire sections are: MAT = 12.25°C; Summer Temperature = 20.22°C; Winter Temperature = 4.05°C.

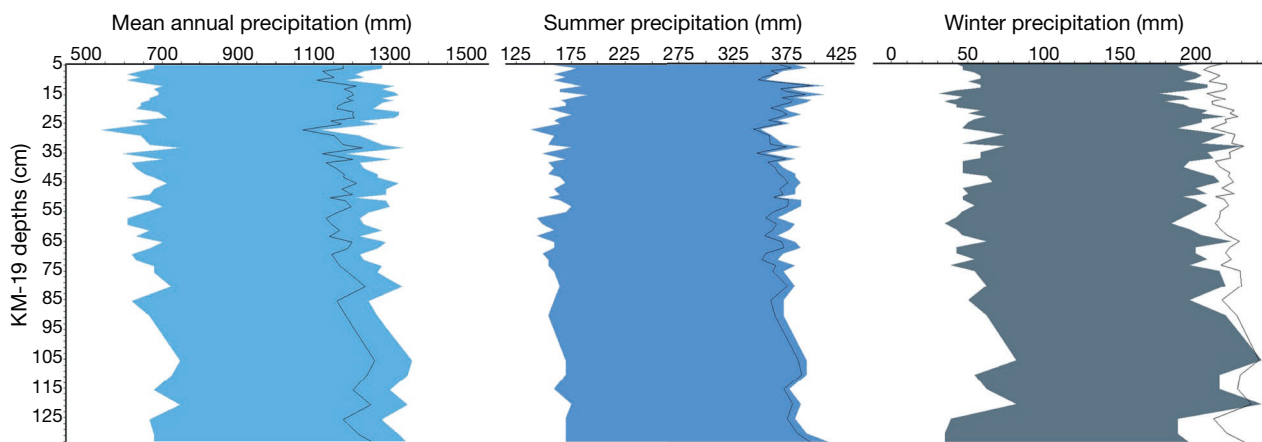


Fig. 3. — Precipitation reconstructions for the Kenslow Member showing the mean value (black line) and 50% uncertainty intervals (coloured portions). The average values for the entire sections are: MAP = 1179 mm/yr; Summer Precipitation = 369 mm; Winter Precipitation = 220 mm. Note that the mean value lies towards the upper 50% uncertainty interval (and above for Winter precipitation) as the probability density curves are skewed towards higher precipitation (long tails to the curves towards lower precipitation caused by family-level nearest living relative assignments).

McCoy *et al.* (2022) was sample normalised to account for different total palynomorph count sizes and then the whole dataset was subjected to a Box-Cox Transformation in PAST 4.14 (Hammer *et al.* 2001). The transformed data was then ordinated in a cluster analysis using Euclidean distance to group palynomorph taxa. The resulting dendrogram groups taxa with similar data patterns in the dataset. This led to five clusters which are herein termed Groups 1 to 5 (Table 1). The pollen and spore sum for each group was then calculated for each sample.

ANALYSIS

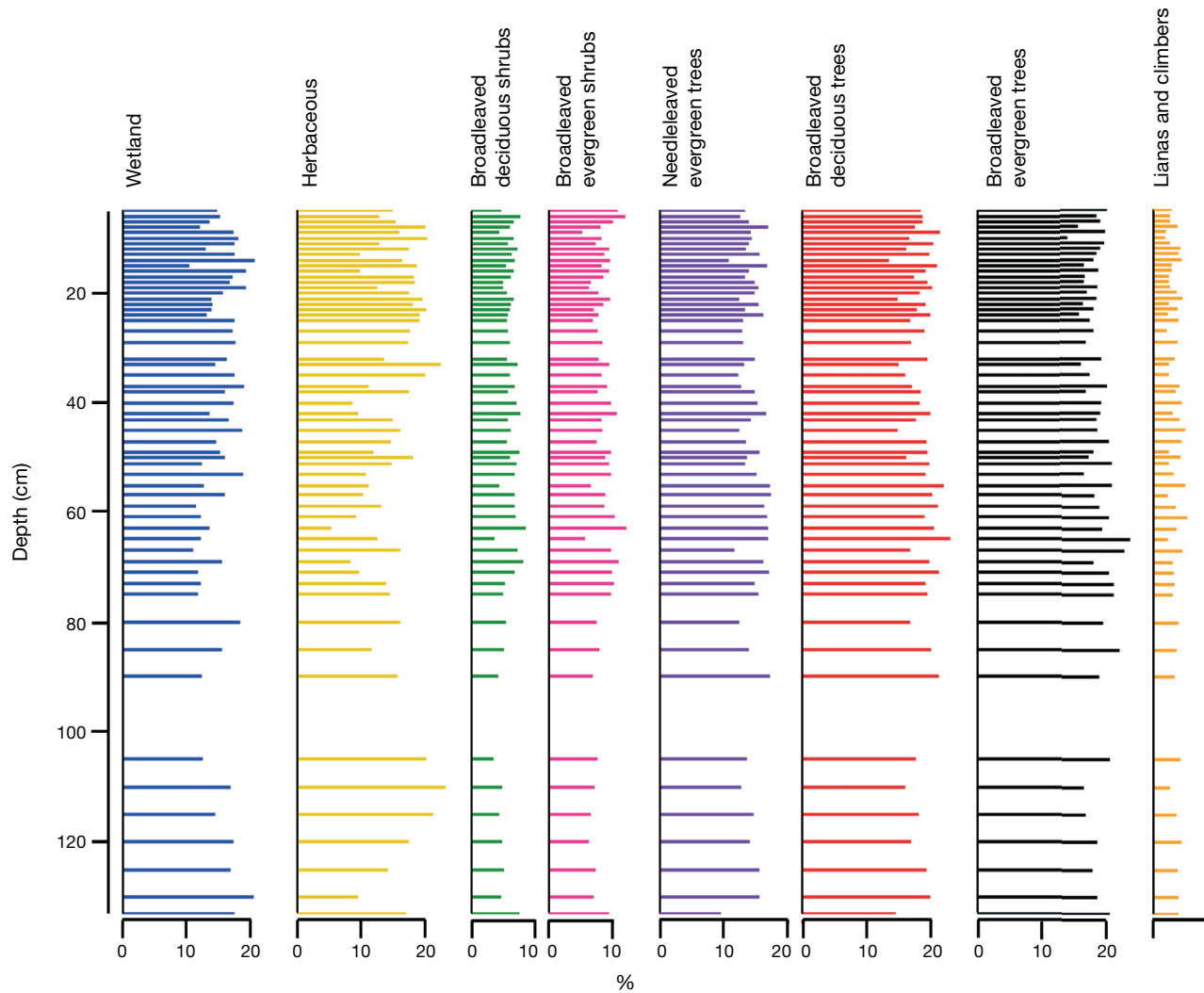
Pearson's Correlation was then used to compare the palaeoclimate, PFT and Group results. This analysis was performed in PAST 4.14 (Hammer *et al.* 2001). Although this correlation coefficient only compares the change in two datasets and offers no indication of causality, it is possible to infer a logical causality between our three datasets: climate is the likely

driver of changes in PFT and Group data (although plants can certainly impact climate at a variety of scales e.g. Notaro *et al.* [2006] and D'Odorico *et al.* [2013]). Any correlation between PFTs and Groups is due to the same data being categorised differently and offers insight into the dominant PFTs in the context of the cluster analysis defined groups. For reporting the correlation coefficients, weak correlation is considered to be 0.3–0.39, moderate is 0.4–0.49, strong is 0.5–0.75 and very strong >0.75. All correlation coefficients are presented in Table 2, but only those falling into one of the previously defined categories are reported in the results.

RESULTS

PALAEOCIMATE

The new palaeoclimate reconstructions are presented as the mean value and the values at the 50% uncertainty intervals. Across the 128 cm record (Fig. 1), MAT ranges from 14.14°C (10.92–17.55°C) to 11.48°C (8.32–13.99°C) (Fig. 2; SI 1).

FIG. 4. — Plant functional types of the Kenslow Member groupings following Utescher *et al.* (2021b).

Summer Temperature reconstructions range from 21.58°C (19.35-24.84°C) to 19.52°C (16.92-22.49°C) and Winter Temperature from 6.38°C (2.33-11.44°C) to 2.64°C (-1.42-5.76°C). All temperature reconstructions show a cooling in the mean value from 133 cm to 120 cm before warming again towards 85 cm (Fig. 2). Above average (the average for the entire section: MAT = 12.25°C; Summer Temperature = 20.22°C; Winter Temperature = 4.05°C) temperatures are also reconstructed at 59-57 cm, 38-37 cm, 27 cm and finally from 22-12 cm (Fig. 2). The onset of this final period of above average temperatures coincides with the change in lithology from clay to lignite (McCoy *et al.* 2022).

MAP reconstructions range from 1260 mm/yr (679-1347 mm/yr) to 1071 mm/yr (541-1117 mm/yr) with an average across the section of 1179 mm/yr (Fig. 3). Intervals of above average MAP is present from 133-90 cm, 67-65 cm, 23-21 cm and 16-12 cm (Fig. 3). The lowest reconstructed MAP is recorded at 27 cm and coincides with a warm point in the reconstruction (Figs 2; 3). Summer Precipitation ranges from 399 mm (186-409 mm)

to 343 mm (138-351 mm) with an average of 369 mm (Fig. 3). Above average Summer Precipitation is present from 133-120 cm and 18-11 cm. Winter Precipitation ranges from 241 mm (82-243 mm) to 205 mm (47-192 mm), with an average of 220 mm. The mean value being above the upper 50% uncertainty level shows the skew in the reconstructions and the long tail in the probability density function curve (probably caused by family-level nearest living relative assignments), the optima (mid-point of the probability curve) falls at 109 mm for the lowest Winter Precipitation reconstruction (SI 1). There is an overall trend towards lower Winter Precipitation up section (Fig. 3). Both Summer and Winter Precipitation reconstructions also show the low point at 27 cm, coincident with MAP and higher temperatures (Fig. 2; 3). Although there is some stratigraphical overlap between the above average MAP (16-12 cm) and Summer Precipitation (18-11 cm), this is not present in the Winter Precipitation (Fig. 3). Instead, Winter Precipitation is below average for the entire lignite portion of the section (Fig. 3).

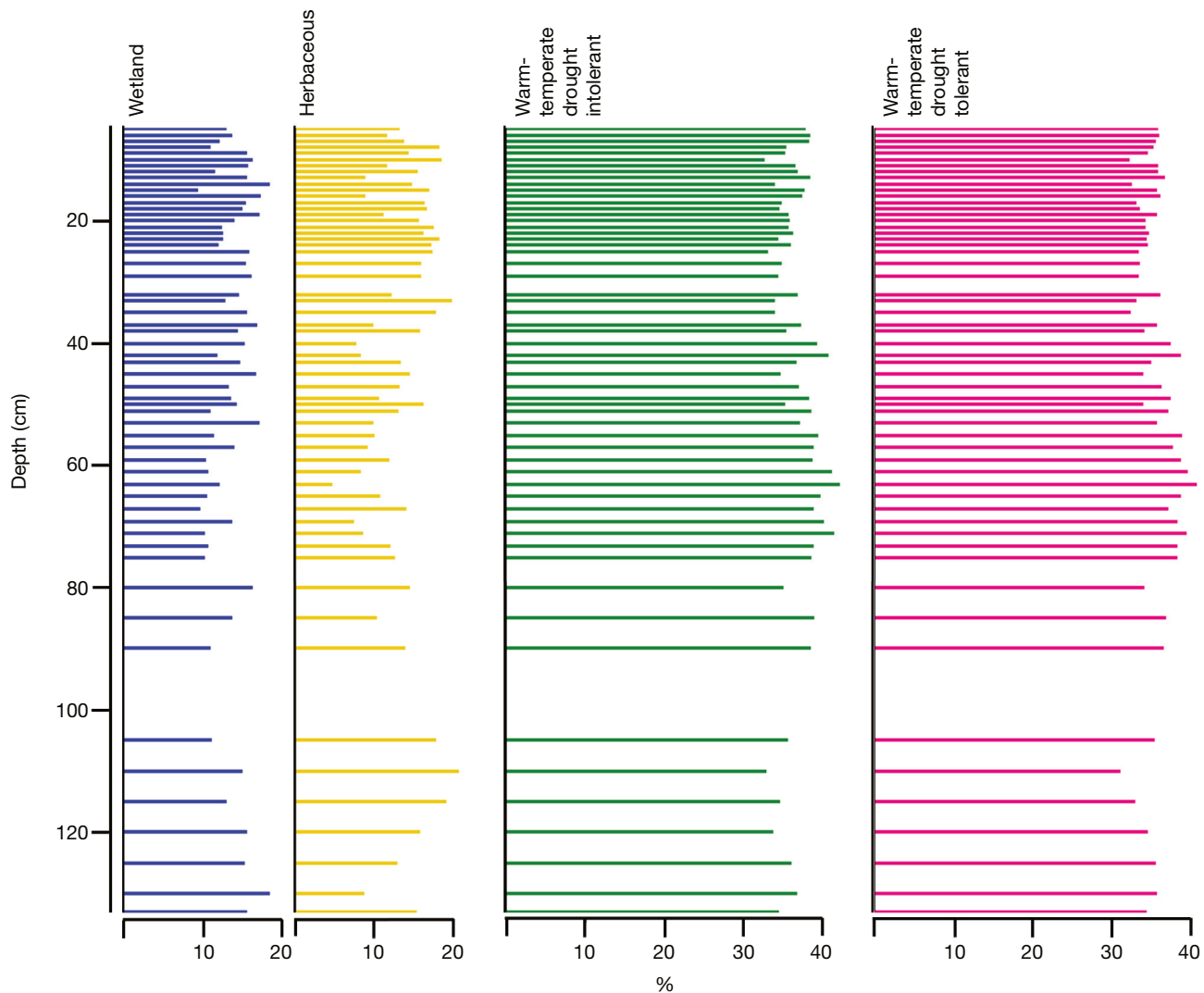


FIG. 5. — Plant functional types of the Kenslow Member grouped by their drought tolerance.

PFTs AND GROUPS

The dominant PFTs are Broadleaved evergreen trees (14.15-23.70%) and broadleaved deciduous trees (13.55-23.00%), followed by Wetland (10.42-20.53%), needleleaf evergreen trees (9.58-17.34%) and Herbaceous (5.31-23.11%) (Fig. 4). The other three PFT groups are present throughout in smaller proportions: broadleaved evergreen shrubs reach a maximum proportion of 12.02%, broadleaved deciduous shrubs highest value is 8.57% and lianas and climbers are present at less than 5.33% (Fig. 4). Broadleaved evergreen trees are dominant until 27 cm, after which broadleaved deciduous trees more frequently dominate (Fig. 4). Decreases in the proportion of broadleaved evergreen trees below 27 cm depth are often at the expense of either needleleaved evergreen trees or herbaceous plants (Fig. 4). Herbaceous elements gain their greatest proportion at 110 cm, 35-33 cm, 29-20 cm and 10-7 cm depth (Fig. 4). Wetland taxa decrease from 130-59 cm, before increasing towards 25 cm depth (Fig. 4). A low proportion of Wetland taxa from 25-21 cm is followed

by increased proportions through the lignite to 8 cm. There is no dominance between either drought tolerant or intolerant PFTs throughout the section (Fig. 5).

The cluster defined groups show a dominance of Group 4 throughout the section, except in samples at 15 cm, 12 cm and 7 cm (Fig. 6; Table 1). Group 4 also shows a decreasing trend towards the top of section (Fig. 6). Group 1 is initially absent, or present as less than 3% of the assemblages, until 80 cm depth, after which it increases to 30% of samples before decreasing towards the top of section (Fig. 6). Group 2 increases in relative abundance from 42 cm to the top of section (Fig. 6). Before this, it is typically present at relative abundances greater than 5%, although Group 2 is nearly absent from assemblages between 71-61 cm depth (Fig. 6). Group 3 is present throughout the section in relative abundances of between 5% and 25%, except from 75-55 cm depth (Fig. 6). Group 5 decreases in abundance from 85-63 cm depth, before increasing from 9% at 63 cm to 41% at 7 cm depth (Fig. 6).

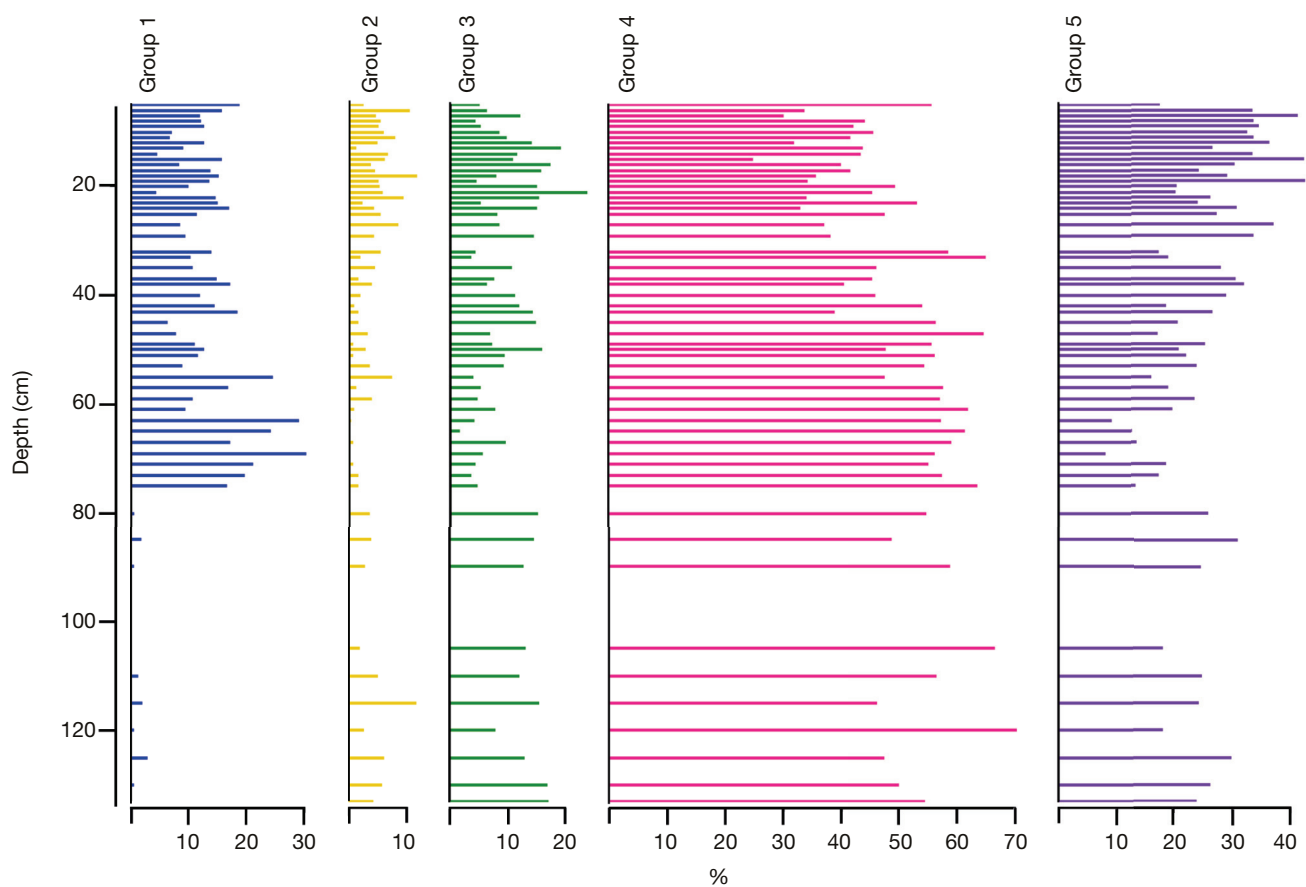


FIG. 6. — Cluster analysis defined groupings of Kenslow Member pollen and spores.

CORRELATION BETWEEN CLIMATE AND VEGETATION

Unsurprisingly, paired temperature variables are very strongly positively correlated and paired precipitation variables are very strongly and strongly positively correlated (Table 2). This is except for Summer Precipitation and Winter Precipitation, which are not correlated (Table 2). Winter Temperature and Winter Precipitation are strongly negatively correlated, whereas Summer Temperature and Summer Precipitation are moderately positively correlated (Table 2). Groups 2 and 4 are weakly positively correlated with MAT (Table 2). Summer Temperature does not correlate with any PFT or cluster group. Winter Temperature is strongly negatively correlated with Group 4 and moderately positively correlated with Group 2. MAP is weakly positively correlated with the lianas and climbers PFT and weakly negatively correlated with broadleaved deciduous trees and needleleaved evergreen trees PFTs (Table 2). Winter Precipitation is strongly positively correlated with Group 4 and weakly negatively correlated with broadleaved deciduous tree PFTs. Summer Precipitation is weakly positively correlated with Group 3 and weakly negatively correlated with needleleaved evergreen trees (Table 2).

Pearson's Correlation shows that cluster Groups 4 and 5 are very strongly negatively correlated (Table 2; Fig. 6). Groups 2 and 4, Groups 1 and 3, and Groups 2 and 5 are strongly negatively correlated. Group 4 is moderately positively correlated with broadleaved evergreen tree PFTs and Group 2 is moderately negatively correlated with broadleaved evergreen tree PFTs, suggesting this is the control behind their proportional relationship (Fig. 6; Table 2). Group 2 is also weakly positively correlated with herbaceous PFTs, whereas Group 5 is weakly negatively correlated with broadleaved evergreen tree PFTs (Table 2). Group 1 (positive correlation) and Group 3 (negative correlation) are associated with needleleaved evergreen tree and broadleaved deciduous tree PFTs (Table 2). Group 1 is also weakly negatively correlated with herbaceous and wetland PFTs (Table 2).

DISCUSSION

HOW DRY AND SEASONAL WAS EUROPE DURING THE SERRAVALLIAN?

Conflicting proxy results and modelling studies have proposed varying degrees of humidity and aridity for the Serravallian of Europe (van Dam 2006; Böhme *et al.* 2008; Bruch *et al.*

2011; Methner *et al.* 2020; Botsyun *et al.* 2022). Most of these previous studies have focussed on central European basins and basins around the Alps (Böhme *et al.* 2008; Bruch *et al.* 2011; Methner *et al.* 2020; Botsyun *et al.* 2022). For the Serravallian, palaeobotany using the Co-existence Approach reconstructs 850–1500 mm/yr across Central and Eastern Europe (Bruch *et al.* 2011; McCoy *et al.* 2022), rodent faunas show most of Europe (outside of the Iberian Peninsula and Anatolia) to have received over 800–1300 mm/yr (van Dam 2006), while herpetofaunas reconstruct 0–900 mm/yr for Central and Eastern Europe (Böhme *et al.* 2008). However, as it is highly unlikely that the whole of Europe ever received 0 mm/yr for an extended period of the Serravallian, the herpetofauna reconstruction (lower estimate) is not considered robust (Böhme *et al.* 2008). The new results from the Kenslow Member, whilst outside of the regions most extensively studied in the past, show a comparable MAP to rodent and Co-existence Approach reconstructions (Fig. 3). Taking into account the 50% uncertainty interval on the new results and the +275 mm uncertainty reported for the herpetofauna-based reconstructions, shows remarkable overlap between all proxies in the region of 900–1200 mm/yr for most of mid-latitude Europe during the Serravallian (van Dam 2006; Böhme *et al.* 2008; Bruch *et al.* 2011). Even if we take the contrary position that this overlap is entirely due to the chance overlap of uncertainty, it is not unexpected to have different areas in a geographical region with variable rainfall (Lundqvist & Falkenmark 2010). Therefore, should we even be asking the question of was Europe dry during the Miocene? No, we shouldn't. Only comparison with geographically widespread proxy data will help us understand this dynamic variable in deep time.

Our results show the presence of a humid climate in the United Kingdom during the Serravallian that agrees with previous reconstructions (Gibson *et al.* 2022; McCoy *et al.* 2022; Pound *et al.* 2022). Summers are reconstructed marginally more humid than winters in agreement with Bruch *et al.* (2011), but not substantially enough to shift the Koppen-Geiger classification to a summer wet designation – in agreement with fossil fungal evidence (Pound *et al.* 2022). In Europe, the Serravallian hydrology has been proposed to be controlled by westerly winds delivering moisture across the central basins, especially during winter (Quan *et al.* 2014; Methner *et al.* 2020). It is also likely that the more oceanic position of the United Kingdom would have created a different hydrological regime to central Europe, especially following the contraction of substantial water masses of eastern Europe (Piller *et al.* 2007) and considering that modelling of palaeo-waterbodies shows they could have provided a localised increase in precipitation (Pound *et al.* 2014).

THE SERRAVALLIAN CLIMATE AND BIOME OF THE UNITED KINGDOM

Based on these new reconstructed mean values, the Kenslow Member records a Cfb (temperate, no dry season with a warm summer) Koppen-Geiger classification. All summer temperatures could fall into the Cfa (hot summer) Koppen-Geiger classification when the 50% uncertainty intervals are

		Lianas and Climbers									
		Broadleaved evergreen trees					Broadleaved deciduous trees				
		Needleleaved evergreen trees					Broadleaved evergreen shrubs				
		Broadleaved deciduous shrubs					Herbaceous				
		Wetland					Winter Precipitation				
		Summer Precipitation					Mean Annual Precipitation				
		Winter Temperature					Summer Temperature				
		Mean Annual Temperature					Mean Annual Temperature				
		Group 5					Group 4				
		Group 3					Group 2				
		Group 4					Group 1				
Group 1	-0.233771	-0.547930	-0.113635	-0.276478	-0.146316	-0.207692	-0.137656	-0.403299	-0.346783	-0.288032	-0.372488
Group 2	0.203860	-0.569180	0.541978	0.341292	0.155909	0.424343	-0.087980	0.139733	-0.369171	0.211123	0.381642
Group 3	-0.299494	0.242064	0.191553	0.222116	0.167178	0.267511	0.318498	0.122084	0.281220	0.198542	0.015680
Group 4	-0.796860	-0.377806	-0.101515	-0.507028	0.341266	-0.024767	0.607783	-0.189641	-0.175526	-0.024285	0.115739
Group 5	0.079791	0.035492	0.204333	-0.011649	0.030707	-0.053223	0.120454	0.099533	-0.060582	-0.099012	-0.049649
Mean Annual Temperature	0.906524	0.969246	-0.070822	0.244628	-0.445305	0.148392	-0.153054	0.148392	-0.153054	0.197996	0.141355
Summer Temperature	0.786485	0.168849	0.417308	-0.191784	0.148108	-0.198294	0.189294	0.208615	0.208615	0.208634	0.208634
Winter Temperature	-0.222446	0.108468	-0.537719	0.174834	-0.169398	-0.169398	-0.169398	-0.089282	-0.089282	-0.089282	-0.089282
Mean Annual Precipitation	0.837066	0.689170	0.049081	0.193409	-0.167128	-0.091793	-0.167128	-0.311880	-0.311880	-0.311880	-0.311880
Summer Precipitation	0.292287	0.039424	0.218021	-0.063124	-0.033931	-0.312360	-0.312360	-0.299068	-0.299068	-0.299068	-0.299068
Winter Precipitation	-0.040214	0.218020	-0.171561	-0.105102	-0.218899	-0.307560	-0.307560	-0.197507	-0.197507	-0.197507	-0.197507

taken into account (Fig. 2). Today central England still classifies as Cfb Köppen-Geiger classification (Beck *et al.* 2018). However, the present-day MAT of Bees Nest Pit is 7.98°C with a Summer Temperature of 13.71°C and a Winter Temperature of 2.98°C (Fick & Hijmans 2017). The Serravallian of the United Kingdom was around 5°C warmer annually, with pronounced summer warming (+6.5°C) and a slightly warmer winter (+1°C). Today the average rainfall at Bees Nest Pit is MAP = 1042 mm/yr Summer Precipitation = 236 mm and Winter Precipitation = 285 mm (Fick & Hijmans 2017). This shows the Serravallian climate of the United Kingdom had around 10% more precipitation across the year, but this rainfall was more concentrated in the summer with 31% of the annual amount falling in these three months, rather than the 22% in the present climate. In contrast today's climate has just over a quarter of the annual total fall in the three months of winter. Whereas in the Serravallian, less than 20% of annual precipitation fell during the winter. This slight seasonality in the present-day precipitation regime is the result of high-pressure westerlies and east moving polar jet streams that are strongest in winter and spring – delivering more precipitation to the United Kingdom (Mayes 1991, 1996). It has previously been proposed that this climate regime initiated during the Serravallian (Quan *et al.* 2014; Pound & Riding 2016). As the Serravallian Bees Nest Pit palynology reconstructs a moderately summer-wet climate, rather than the present-day winter-wet, it likely predates the onset of significant westerlies (Quan *et al.* 2014).

The MAT and MAP reconstructions place the Kenslow Member flora into the Temperate Forest of Whittaker's (1970) biome classification and the Warm Temperate Moist Forest of Holdridge's (1947) biome classification. For Whittaker's (1970) scheme, the 50% uncertainty intervals could place the flora into the Temperate Woodland classification due to the skew in the probability density curve (Fig. 3). MAT and MAP reconstructions (Fig. 2; 3) are consistent with the present-day mixed forests of subtropical China (Ge & Xie 2017) and this interpretation is supported by similar values of broadleaved evergreen tree PFTs, broadleaved deciduous tree PFTs and smaller proportions of needleleaved evergreen tree PFTs (Fig. 6). The reconstructed climate variables for the Serravallian Kenslow Member at Bees Nest Pit show the presence of a temperate climate with warm summers and no dry season (Fig. 2; 3). This agrees with the fossil fungi reconstructions from the same section (Pound *et al.* 2022) and Co-existence Approach reconstructions (McCoy *et al.* 2022). However, reconstructed MAT is lower than that presented by McCoy *et al.* (2022). Lower MAT reconstructions by *crestr*, when compared to the Co-existence Approach, have been previously reported and likely stem from different modern data used in the reconstruction (Gibson *et al.* 2022).

The statistically identified groupings differ from those qualitatively identified by McCoy *et al.* (2022). The dominance of Group 4 can be explained by the high amounts of *Tsuga* (Endl.) Carrière pollen in this record and the positive correlation with Winter Precipitation likely reflects their dependency on precipitation (Fusco 2010; Xiao *et al.* 2024). Interest-

ingly, Winter Precipitation has a more significant role in the present-day distribution of *Tsuga* species in North America, as opposed to the significance of Summer Precipitation on East Asian *Tsuga* species (Xiao *et al.* 2024). This would imply that the Miocene *Tsuga* species of the United Kingdom were closer in bioclimatic requirements to those of North America. Previous work on European *Tsuga* fossils has identified greater morphological similarities to those from East Asia (Mai & Walther 1978, 1991; Xiao *et al.* 2024). This disparity between reconstructed bioclimatic controls here, and previous morphological studies requires further work to understand the evolutionary placement of extinct European conifers.

Group 4 is strongly negatively correlated with Group 5 (Table 2) and visually it is the decrease in Group 4 and the increase in Group 5 that dominates the changes towards the top of the section (Fig. 3). Group 5 is not correlated with any climatic factor and the increase in Group 5 begins lower in section than the onset of lignite formation and below the pollen zonation change identified by McCoy *et al.* (2022). It is therefore unknown what Group 5 is responding to, but it could be speculated to be either successional (Schneider 1992; McCoy *et al.* 2022) or another abiotic aspect.

Group 1 also shows no correlation with climatic factors (Table 2). In contrast to the more diverse Group 5, Group 1 comprises only the anemophilous *Abies* Mill. and *Pinus* L. pollen (Table 1) and it is therefore likely this group represents long-distance transport into the depositional environment. Both are known to travel substantial distances (Yu *et al.* 2004; Poska & Pidek 2010; Ertl *et al.* 2012), although *Abies* transport distances may be more species specific (Yu *et al.* 2004; Poska & Pidek 2010). This type of analysis could therefore provide a more objective means to eliminate extra-local taxa from palaeoclimate reconstructions, should that be desirable (Reichgelt *et al.* 2023).

From the perspective of PFTs, it is clear that MAP is the most important variable: lianas and climbers show positive correlation, whilst broadleaved deciduous trees and needleleaved evergreen trees show negative correlation (Table 2). Both these latter PFTs show negative correlation with seasonal rainfall, broadleaved deciduous trees negatively correlate with Winter Precipitation, whereas needleleaved evergreen trees negatively correlate with Summer Precipitation (Table 2). This may relate to summer water availability that favours broadleaved taxa (Harvey *et al.* 2020) and the longer growing season provided by mild Winter Precipitation that can benefit evergreen trees (Box & Fujiwara 2015).

CONCLUSIONS

The new palaeoclimate reconstructions for the Kenslow Member palynoflora show an oceanic type climate with no pronounced dry season. However, more rainfall fell during the summer than the winter. This contrasts with the present-day, implying that the high-pressure westerlies and east moving polar jet stream that controls the rainfall regime today was not as important. The unique assemblage recorded in the

Kenslow Member shows that seasonal availability of moisture was a crucial control on the reproducing plant community. The correlation between Winter Precipitation and *Tsuga* pollen, suggests these probably extinct taxa had bioclimatic responses more like their extant North American relatives. This is in contradiction with proposed morphological similarities between European *Tsuga* macrofossils and extant East Asian species.

Acknowledgements

The fieldwork was funded by an Elspeth Matthews Fund granted by the Geological Society of London to Matthew Pound in 2019. Matthew Pound thanks NERC (NE/V01501X/1) and The Royal Society (IEC\R2\202086) for funding. Jennifer M.K. O'Keefe thanks NSF (award #2015813). James B. Riding publishes with the approval of the Executive Director, British Geological Survey (NERC). We are grateful to Anaïs Boura and Cédric Del Rio for their insightful reviews. We thank Emmanuel Côtez for all their support as editor.

REFERENCES

ACOSTA R. P., BURLS N. J., POUND M. J., BRADSHAW C. D., DE BOER A. M., HEROLD N., HUBER M., LIU X., DONNADIEU Y., FARNSWORTH A., FRIGOLA A., LUNT D. J., VON DER HEYDT A. S., HUTCHINSON D. K., KNORR G., LOHMAN G., MARZOCCHI A., PRANGE M., SARR A. C., LI X. & ZHANG Z. 2024a. — A Model-Data Comparison of the Hydrological Response to Miocene Warmth: Leveraging the Miomip1 Opportunistic Multi-Model Ensemble. *Paleoceanography and Paleoclimatology* 39: e2023pa004726. <https://doi.org/10.1029/2023pa004726>

ACOSTA R. P., BURLS N. J., POUND M. J., BRADSHAW C. D., MCCOY J., GIBSON M., O'KEEFE J. M. K. & FEAKINS S. J. 2024b. — Climate conundrum: A wet or dry European and Northern African climate during the middle Miocene. *Geophysical Research Letters* 51: e2024gl109499. <https://doi.org/10.1029/2024gl109499>

BECK H. E., ZIMMERMANN N. E., MCVICAR T. R., VERGOPOLAN N., BERG A. & WOOD E. F. 2018. — Present and future Köppen-Geiger climate classification maps at 1-km resolution. *Scientific Data* 5: 1-12. <https://doi.org/10.1038/sdata.2018.214>

BÖHME M., ILG A. & WINKLHOFER M. 2008. — Late Miocene “washhouse” climate in Europe. *Earth and Planetary Science Letters* 275: 393-401. <https://doi.org/10.1016/j.epsl.2008.09.011>

BOTSYUN S., EHRLERS T. A., KOPTEV A., BÖHME M., METHNER K., RISI C., STEPANEK C., MUTZ S. G., WERNER M., BOATENG D. & MULCH A. 2022. — Middle Miocene climate and stable oxygen isotopes in Europe based on numerical modeling. *Paleoceanography and Paleoclimatology* 37: e2022pa004442. <https://doi.org/10.1029/2022pa004442>

BOULTER M. C., FORD T. D., IJTABA M. & WALSH P. T. 1971. — Brasington Formation: a newly recognized Tertiary Formation in the southern Pennines. *Nature Physical Science* 231: 134-136. <https://doi.org/10.1038/physci231134a0>

BOX E. O. & FUJIWARA K. 2015. — Warm-temperate deciduous forests: concept and global overview, in BOX E. O. & FUJIWARA K. (eds), *Warm-temperate deciduous forests around the Northern hemisphere*. Springer, Cham: 7-26. https://doi.org/10.1007/978-3-319-01261-2_2

BRUCH A. A., UTESCHER T. & MOSBRUGGER V. 2011. — Precipitation patterns in the Miocene of Central Europe and the development of continentality. *Palaeogeography, Palaeoclimatology, Palaeoecology* 304: 202-211. <https://doi.org/10.1016/j.palaeo.2010.10.002>

CHEVALIER M. 2019. — Enabling possibilities to quantify past climate from fossil assemblages at a global scale. *Global and Planetary Change* 175: 27-35. <https://doi.org/10.1016/j.gloplacha.2019.01.016>

CHEVALIER M. 2022a. — crestr: an R package to perform probabilistic climate reconstructions from palaeoecological datasets. *Climate of the Past* 18: 821-844. <https://doi.org/10.5194/cp-18-821-2022>

CHEVALIER M. 2022b. — mchevalier2/crestr: v1.0.1. *Zenodo*. <https://doi.org/10.5281/zenodo.6458405>

CHEVALIER M., CHEDDADI R. & CHASE B. M. 2014. — Crest (Climate Reconstruction SoftWare): a probability density function (Pdf)-based quantitative climate reconstruction method. *Climate of the Past* 10: 2081-2098. <https://doi.org/10.5194/cp-10-2081-2014>

D'ODORICO P., HE Y., COLLINS S., DE WEKKER S. F., ENGEL V. & FUENTES J. D. 2013. — Vegetation–microclimate feedbacks in woodland–grassland ecotones. *Global Ecology and Biogeography* 22: 364-379. <https://doi.org/10.1111/geb.12000>

EDINA 2024. — High Resolution (25 cm) Vertical Aerial Imagery [JPG geospatial data], Scale 1:500, Tiles: sk2555, sk2553, sk2255, sk2355, sk2354, sk2353, sk2455, sk2454, sk2453, sk2254, sk2253, sk2155, sk2154, sk2153. Updated: 28 October 2022, Getmapping, Using: Edina Aerial Digimap Service [retrieved from <https://digimap.edina.ac.uk> on 23 June, 2024].

ERTL C., PESSI A. M., HUUSKO A., HICKS S., KUBIN E. & HEINO S. 2012. — Assessing the proportion of “extra-local” pollen by means of modern aerobiological and phenological records – An example from Scots pine (*Pinus sylvestris* L.) in northern Finland. *Review of Palaeobotany and Palynology* 185: 1-12. <https://doi.org/10.1016/j.revpalbo.2012.07.014>

ESCOBAR-TORREZ K., FRANCO CASSINO R. & LEDRU M. P. 2024. — Relationship between pollination syndromes, pollen morphology and plant ecology in Quaternary deposits of the Cerrado. *Palynology* 48: 2252871. <https://doi.org/10.1080/01916122.2023.2252871>

FICK S. E. & HIJMANS R. J. 2017. — WorldClim 2: new 1-km spatial resolution climate surfaces for global land areas. *International Journal of Climatology* 37: 4302-4315. <https://doi.org/10.1002/joc.5086>

FORSTER P., STORELVMO T., ARMOUR K., COLLINS W., DUFRESNE J.-L., FRAME D., LUNT D. J., MAURITSEN T., PALMER M. D., WATANABE M., WILD M. & ZHANG H. 2021. — The Earth's Energy Budget, Climate Feedbacks, and Climate Sensitivity, in MASSON-DELMOTTE V., ZHAI P., PIRANI A., CONNORS S. L., PÉAN C., BERGER S., CAUD N., CHEN Y., GOLDFARB L., GOMIS M. I., HUANG M., LEITZELL K., LONNOY E., MATTHEWS J. B. R., MAYCOCK T. K., WATERFIELD T., YELEKÇİ O., YU R. & ZHOU B. (eds), *Climate Change 2021: The Physical Science Basis. Contribution of Working Group I to the Sixth Assessment Report of the Intergovernmental Panel on Climate Change*. Cambridge University Press, Cambridge and New York: 923-1054. <https://doi.org/10.1017/9781009157896.009>

FRANÇOIS L., UTESCHER T., FAVRE E., HENROT A. J., WARNANT P., MICHEELS A., ERDEI B., SUC J. P., CHEDDADI R. & MOSBRUGGER V. 2011. — Modelling Late Miocene vegetation in Europe: Results of the Caraib model and comparison with palaeo-vegetation data. *Palaeogeography, Palaeoclimatology, Palaeoecology* 304: 359-378. <https://doi.org/10.1016/j.palaeo.2011.01.012>

FUSCO F. 2010. — *Picea* + *Tsuga* pollen record as a mirror of oxygen isotope signal? An insight into the Italian long pollen series from Pliocene to Early Pleistocene. *Quaternary International* 225: 58-74. <https://doi.org/10.1016/j.quaint.2009.11.038>

GBIF 2020a. — Gbif.org (Date accessed: 24 September 2020) Liliopsida occurrence data. <https://doi.org/10.15468/dl.axv3y3d>

GBIF 2020b. — Gbif.org (Date accessed: 24 September 2020) Lycopodiopsida occurrence data. <https://doi.org/10.15468/dl.ydhyhz>

GBIF 2020c. — Gbif.org (Date accessed: 24 September 2020) Magnoliopsida occurrence data. <https://doi.org/10.15468/dl.ra49dt>

GBIF 2020d. — Gbif.org (Date accessed: 24 September 2020) Pinopsida occurrence data. <https://doi.org/10.15468/dl.x2r7pa>

GBIF 2020e. — Gbif.org (Date accessed: 24 September 2020) Polypodiopsida occurrence data. <https://doi.org/10.15468/dl.87tbp6>

GE J. & XIE Z. 2017. — Geographical and climatic gradients of evergreen versus deciduous broad-leaved tree species in subtropical China: Implications for the definition of the mixed forest. *Ecology and Evolution* 7: 3636-3644. <https://doi.org/10.1002/ece3.2967>

GIBSON M. E., MCCOY J., O'KEEFE J. M. K., NUÑEZ OTAÑO N. B., WARNY S. & POUND M. J. 2022. — Reconstructing terrestrial paleoclimates: a comparison of the co-existence approach, bayesian and probability reconstruction techniques using the UK Neogene. *Paleoceanography and Paleoclimatology* 37: e2021pa004358. <https://doi.org/10.1029/2021pa004358>

HAMMER Ø., HARPER D. A. T. & RYAN P. D. 2001. — Past: Paleontological statistics software package for education and data analysis. *Palaeontologia Electronica* 4: 1-9. http://palaeo-electronica.org/2001_1/past/issue1_01.htm

HARVEY J. E., SMILJANI M., SCHARNWEBER T., BURAS A., CEDRO A., CRUZ-GARCÍA R., DROBYSHEV I., JANECKA K., JANSONS Å., KACZKA R. & KLISZ M. 2020. — Tree growth influenced by warming winter climate and summer moisture availability in northern temperate forests. *Global Change Biology* 26: 2505-2518. <https://doi.org/10.1111/gcb.14966>

HOLDRIDGE L. R. 1947. — Determination of world plant formations from simple climatic data. *Science* 105: 367-368. <https://doi.org/10.1126/science.105.2727.367>

LUNDQVIST J. & FALKENMARK M. 2010. — Adaptation to rainfall variability and unpredictability: New dimensions of old challenges and opportunities. *International Journal of Water Resources Development* 26: 595-612. <https://doi.org/10.1080/07900627.2010.519488>

MAI D. H. & WALTHER H. 1978. — Die Floren der Haselbacher Serie im Weißelster-Becken (Bezirk Leipzig, DDR). *Abhandlungen des Staatlichen Museums für Mineralogie und Geologie zu Dresden* 28: 1-200.

MAI D. H. & WALTHER H. 1991. — Die oligozänen und untermiozänen Floren Nordwest-Sachsens und des Bitterfelder Raumes. *Abhandlungen des Staatlichen Museums für Mineralogie und Geologie zu Dresden* 38: 1-230.

MAYES J. 1991. — Regional airflow patterns in the British Isles. *International Journal of Climatology* 11 (5): 473-491. <https://doi.org/10.1002/joc.3370110502>

MAYES J. 1996. — Spatial and temporal fluctuations of monthly rainfall in the British Isles and variations in the mid-latitude westerly circulation. *International Journal of Climatology* 16: 585-596. [https://doi.org/10.1002/\(SICI\)1097-0088\(199605\)16:5%3C585::AID-JOC24%3E3.0.CO;2-2%23](https://doi.org/10.1002/(SICI)1097-0088(199605)16:5%3C585::AID-JOC24%3E3.0.CO;2-2%23)

MCCOY J., BARRASS-BARKER T., HOCKING E. P., O'KEEFE J. M. K., RIDING J. B. & POUND M. J. 2022. — Middle Miocene (Serravallian) wetland development on the northwest edge of Europe based on palynological analysis of the uppermost Brassington Formation of Derbyshire, United Kingdom. *Palaeogeography, Palaeoclimatology, Palaeoecology* 603: 111180. <https://doi.org/10.1016/j.palaeo.2022.111180>

MCCOY J., GIBSON M. E., HOCKING E. P., O'KEEFE J. M. K., RIDING J. B., ROBERTS R., CAMPBELL S., ABBOTT G. D. & POUND M. J. 2024. — Temperate to tropical palaeoclimates on the northwest margin of Europe during the middle Cenozoic. *Palaeontologia Electronica* 27: 27.2.a43. <https://doi.org/10.26879/1349>

METHNER K., CAMPANI M., FIEBIG J., LÖFFLER N., KEMPF O. & MULCH A. 2020. — Middle Miocene long-term continental temperature change in and out of pace with marine climate records. *Scientific Reports* 10: 7989. <https://doi.org/10.1038/s41598-020-64743-5>

NOTARO M., LIU Z. & WILLIAMS J. W. 2006. — Observed vegetation-climate feedbacks in the United States. *Journal of Climate* 19: 763-786. <https://doi.org/10.1175/Jcli3657.1>

O'KEEFE J. M. K., POUND M. J., RIDING J. B. & VANE C. H. 2020. — Cellular preservation and maceral development in lignite and wood from the Brassington Formation (Miocene), Derbyshire, UK. *International Journal of Coal Geology* 222: 103452. <https://doi.org/10.1016/j.coal.2020.103452>

PILLER W. E., HARZHAUSER M. & MANDIC O. 2007. — Miocene Central Paratethys stratigraphy—current status and future directions. *Stratigraphy* 4: 151-168. <https://doi.org/10.29041/strat.04.2.09>

POSKA A. & PIDEK I. A. 2010. — Pollen dispersal and deposition characteristics of *Abies alba*, *Fagus sylvatica* and *Pinus sylvestris*, Roztocze region (Se Poland). *Vegetation History and Archaeobotany* 19: 91-101. <https://doi.org/10.1007/s00334-009-0230-x>

POUND M. J. & RIDING J. B. 2016. — Palaeoenvironment, palaeoclimate and age of the Brassington Formation (Miocene) of Derbyshire, UK. *Journal of the Geological Society* 173: 306-319. <https://doi.org/10.1144/jgs2015-050>

POUND M. J. & SALZMANN U. 2017. — Heterogeneity in global vegetation and terrestrial climate change during the late Eocene to early Oligocene transition. *Scientific Reports* 7: 43386. <https://doi.org/10.1038/srep43386>

POUND M. J., TINDALL J., PICKERING S. J., HAYWOOD A. M., DOWSETT H. J. & SALZMANN U. 2014. — Late Pliocene lakes and soils: a global data set for the analysis of climate feedbacks in a warmer world. *Climate of the Past* 10: 167-180. <https://doi.org/10.5194/cp-10-167-2014>

POUND M. J., NUÑEZ OTAÑO N. B., ROMERO I. C., LIM M., RIDING J. B. & O'KEEFE J. M. 2022. — The fungal ecology of the Brassington Formation (Middle Miocene) of Derbyshire, United Kingdom, and a new method for palaeoclimate reconstruction. *Frontiers in Ecology and Evolution* 10: 947623. <https://doi.org/10.3389/fevo.2022.947623>

PRENTICE I. C. 1985. — Pollen representation, source area, and basin size: toward a unified theory of pollen analysis. *Quaternary Research* 23: 76-86. [https://doi.org/10.1016/0033-5894\(85\)90073-0](https://doi.org/10.1016/0033-5894(85)90073-0)

QUAN C., LIU Y.-S., TANG H. & UTESCHER T. 2014. — Miocene shift of European atmospheric circulation from trade wind to westerlies. *Scientific Reports* 4: 5660. <https://doi.org/10.1038/srep05660>

REICHGELT T., BAUMGARTNER A., FENG R. & WILLARD D. A. 2023. — Poleward amplification, seasonal rainfall and forest heterogeneity in the Miocene of the eastern USA. *Global and Planetary Change* 222: 104073. <https://doi.org/10.1016/j.gloplacha.2023.104073>

RSTUDIO TEAM 2022. — Rstudio: Integrated Development Environment for R. Rstudio, Pbc, Boston, Ma. <http://www.rstudio.com/>

SCHNEIDER W. 1992. — Floral successions in Miocene swamps and bogs of Central Europe. *Zeitschrift für geologische Wissenschaften* 20: 555-570.

STEINTHORSDOTTIR M., COXALL H. K., DE BOER A. M., HUBER M., BARBOLINI N., BRADSHAW C. D., BURLS N. J., FEAKINS S. J., GASSON E., HENDERIKS J., HOLBOURN A. E., KIEL S., KOHN M. J., KNORR G., KÜRSCHNER W. M.,LEAR C. H., LIEBRAND D., LUNT D. J., MÖRS T., PEARSON P. N., POUND M. J., STOLL H. & STRÖMBERG C. A. E. 2021. — The Miocene: The Future of the Past. *Paleoceanography and Paleoclimatology* 36: e2020pa004037. <https://doi.org/10.1029/2020pa004037>

UTESCHER T., BRUCH A. A., ERDEI B., FRANÇOIS L., IVANOV D., JACQUES F. M. B., KERN A. K., LIU Y. S., MOSBRUGGER V. & SPICER R. A. 2014. — The Coexistence Approach – Theoretical background and practical considerations of using plant fossils for climate quantification. *Palaeogeography, Palaeoclimatology, Palaeoecology* 410: 58-73. <https://doi.org/10.1016/j.palaeo.2014.05.031>

UTESCHER T., ASHRAF A. R., KERN A. K. & MOSBRUGGER V. 2021a. — Diversity patterns in microfloras recovered from Miocene brown coals of the lower Rhine Basin reveal distinct coupling of the structure of the peat-forming vegetation and continental climate variability. *Geological Journal* 56: 768–785. <https://doi.org/10.1002/gj.3801>

UTESCHER T., ERDEI B., FRANÇOIS L., HENROT A. J., MOSBRUGGER V. & POPOVA S. 2021b. — Oligocene vegetation of Europe and western Asia – Diversity change and continental patterns reflected by plant functional types. *Geological Journal* 56: 628–649. <https://doi.org/10.1002/gj.3830>

VAN DAM J. A. 2006. — Geographic and temporal patterns in the late Neogene (12–3 Ma) aridification of Europe: The use of small mammals as paleoprecipitation proxies. *Palaeogeography, Palaeoclimatology, Palaeoecology* 238: 190–218. <https://doi.org/10.1016/j.palaeo.2006.03.025>

WALSH P. T., BANKS V. J., JONES P. F., POUND M. J. & RIDING J. B. 2018. — A reassessment of the Brassington Formation (Miocene) of Derbyshire, UK and a review of related hypogene karst suffusion processes. *Journal of the Geological Society* 175: 443–463. <https://doi.org/10.1144/jgs2017-029>

WHITTAKER R. H. 1970. — Communities and ecosystems. Macmillan, New York, 385 p.

XIAO S., LI S., HUANG J., WANG X., WU M., KARIM R., DENG W. & SU T., 2024. — Influence of climate factors on the global dynamic distribution of *Tsuga* (Pinaceae). *Ecological Indicators* 158: 111533. <https://doi.org/10.1016/j.ecolind.2023.111533>

YU G., KE X., XUE B. & NI J. 2004. — The relationships between the surface arboreal pollen and the plants of the vegetation in China. *Review of Palaeobotany and Palynology* 129: 187–198. <https://doi.org/10.1016/j.revpalbo.2004.01.007>

Submitted on 22 November 2024;
accepted on 17 March 2025;
published on 29 January 2026.

APPENDIX 1. — Supplementary material: **Table S1**, reconstructed palaeoclimate variables with 50% and 95% probability bounds; samples are organised by depth and are presented by variable; **Table S2**, nearest living relative assignment for fossil pollen and spore taxa and how these were mapped to plant functional types. https://doi.org/10.5852/geodiversitas2026v48a1_s1